

# Fabrication of Porous “Clickable” Polymer Beads and Rods through Generation of High Internal Phase Emulsion (HIPE) Droplets in a Simple Microfluidic Device

M. Talha Gokmen,<sup>†,\*</sup> Wim Van Camp,<sup>†</sup> Patrick J. Colver,<sup>‡</sup> Stefan A. F. Bon,<sup>\*,‡</sup> and Filip E. Du Prez<sup>\*,†</sup>

<sup>†</sup>Polymer Chemistry Research Group, Department of Organic Chemistry, Ghent University, Krijgslaan 281 S4 9000 Gent, Belgium and <sup>‡</sup>Department of Chemistry, University of Warwick, Coventry CV4 7AL, U.K.

Received August 21, 2009; Revised Manuscript Received October 25, 2009

**ABSTRACT:** The fabrication of micrometer-sized monodisperse highly porous polymer particles, of both spherical and rodlike shapes, using a simple microfluidic setup is demonstrated. Droplets were generated in a coflow device from a water-in-oil high internal phase emulsion (HIPE), hereby creating a water-in-oil-in-water (W/O/W) emulsion. The individual droplets of monomer HIPE were polymerized downstream in the channel through photopolymerization. The polymer particles produced via this strategy possess very large macropores in comparison with the more conventional porous polymer beads synthesized by inducing in situ phase separation throughout the polymerization process through the use of porogenic solvents. Epoxy-functionalized porous particles made using the HIPE microfluidic method showed superior performance in a consecutive azide and cycloaddition “click”–“click” modification procedure monitored by IR. Our microfluidic approach led to the successful miniaturization of monodisperse submillimeter spherical poly(HIPE) beads, down to diameters of 400  $\mu\text{m}$ . More strikingly is the production of poly(HIPE) rods, which were obtained by using a viscous HIPE, which in coflow emulsification formed an unstable jet that broke up into rodlike sections. These rodlike droplets maintained their shapes throughout the microfluidic channel and did not relax back into spherical droplets, allowing for production of poly(HIPE) rods upon photopolymerization. The nonspherical shape in this case is not determined by confined channel geometries, which to the best of our knowledge is unprecedented as a strategy to produce nonspherical polymer particles with microfluidics.

## Introduction

Porous polymer beads are used in a wide range of applications, such as stationary phases in separation science,<sup>1,2</sup> resins for solid-phase organic and peptide synthesis,<sup>3</sup> ion-exchange resins,<sup>4</sup> scavengers,<sup>5</sup> and supports for enzyme<sup>6</sup> and catalyst<sup>7</sup> immobilization. Pore sizes are commonly classified as micro, meso, and macro, which correspond to < 2, 2–50, and > 50 nm, respectively.<sup>8</sup> Porous polymer beads can have an open or a closed cellular structure, the former being characterized by pore interconnectivity and the latter by isolated pores. The applications mentioned above require an open cellular structure with a specific average pore size and pore size distribution. For example, size exclusion chromatography (SEC) columns packed with porous cross-linked polystyrene beads are capable of separating a mixture of polymer chains into fractions of similar hydrodynamic volume. The packed column performance, which includes factors as polymer chain separation efficiency and back-pressure, strongly depends on the packing efficiency of the beads, which is governed by their particle size distribution as well as the pore size distribution in each individual bead. In solid phase peptide synthesis (SPPS), beads that possess relatively large macropores are useful as throughout the peptide chain-growth process by consecutive couplings of amino acids the internal porous structure becomes more narrowly confined, leading to longer diffusion time scales and potential pore blockage lowering the efficiency of the peptide production process.

Porous beads are generally prepared by suspension polymerization in which monomer droplets, containing porogen(s), are dispersed in water and subsequently polymerized.<sup>9–11</sup> A greener approach is using emulsified water droplets instead of a porogen, thus creating water-in-oil-in-water (W/O/W) double emulsions. One such example is the preparation of water-expandable polystyrene beads.<sup>12,13</sup> Crevecoeur et al. emulsified water in a pre-polymerized mixture of styrene and polystyrene. The high viscosity of this mixture warrants stability of the emulsified water droplets throughout the dispersion process of this emulsion into droplets and their subsequent polymerization, yielding water-droplet containing polystyrene beads. However, this emulsification step involved conventional mixing and emulsification through shear, which has the disadvantage that it does not allow fabrication of monodisperse beads.

The target requirement for regulating bead size distribution is the control of the droplet generation process, that is, the emulsification of the porogen-containing monomer phase. Kawano et al.<sup>14</sup> reported on the fabrication of monodisperse porous polystyrene beads using a Shirasu porous membrane (SPG) as emulsification device. Vincent et al. described the production of large porous suspension beads with a narrow size distribution using a cross-flow membrane as emulsification device in combination with a tubular polymerization reactor.<sup>15</sup> Whereas with these techniques monodisperse spherical porous beads can be obtained, control of the bead shape, i.e., to produce nonspherical particles, cannot readily be achieved.

We are interested to develop methods that allow fabrication of submillimeter-sized cellular polymer beads that have a unimodal

\*To whom correspondence should be addressed: e-mail Filip.DuPrez@UGent.be, Tel +32-9-2644503, Fax +32-9-2644972.

size distribution and have interconnected micrometer-sized pores as we believe their availability would innovate applications as mentioned above. An approach to fabricate highly porous materials that struck our attention is based on the use of high-internal-phase emulsions (HIPE),<sup>16–19</sup> a special type of emulsion where the volume fraction of the dispersed phase exceeds the 0.74 threshold value for monodisperse emulsions and can reach up to 0.99.<sup>20</sup> The continuous phase is commonly solidified, i.e., through polymerization, to turn HIPE into poly(HIPE). This lightweight material possesses much larger pores than common macroporous materials, and commonly open cellular structures are obtained in which the majority of pores are interconnected.<sup>21</sup> Poly(HIPE)s are mostly prepared via a bulk process,<sup>22</sup> thereby yielding a monolith, the shape of which is predetermined by the reaction vessel. Miniaturization for bead manufacturing by using a mold is possible but tedious. The preferred strategy is to disperse the HIPE in water and thus form HIPE droplets (a water-in-oil-in-water (W/O/W) double emulsion) that are subsequently solidified through polymerization. The W/O/W fabrication of polymer beads using HIPEs is only sparsely reported in patents<sup>23,24</sup> and in the open literature,<sup>25–29</sup> and the prepared poly(HIPE) beads are either as small as  $\sim 60$   $\mu\text{m}$  in diameter but polydisperse<sup>26,28,29</sup> or monodisperse but  $\sim 2$  mm in diameter.<sup>27</sup>

Recently, the development of microfluidic techniques employing lab-on-a-chip devices enabled the preparation of porous monodisperse particles in a single setup.<sup>30,31</sup> Microfluidic bead production is an advanced version of suspension polymerization, in which monomer droplets are created one by one in a controlled and reproducible manner. Droplet generation between two immiscible liquid phases can be achieved by various setups such as T-junction,<sup>32</sup> flow focusing,<sup>33</sup> or coflow geometries.<sup>33</sup> By a careful selection of the discrete phase, various particle geometries can be obtained including gel-type nonporous beads,<sup>34</sup> capsules,<sup>28</sup> armored beads through monomer droplets stabilized by solid particles,<sup>35</sup> and porous beads.<sup>30,31,34</sup> Nonspherical polymer particles were also produced through microfluidics by forcing droplets to move through a channel of confined geometry.<sup>34</sup>

In this paper, we describe a methodology to produce poly(HIPE) particles via a microfluidic approach, not only with control of their diameter (submillimeter range) but also of their shape, moving away from traditional spherical beads. Simultaneously, we demonstrate the possibility to modify the chemical functionality of the internal cellular structure by a straightforward postmodification process, demonstrating that the poly(HIPE) beads can find applications in a variety of fields. To the best of our knowledge, polymerization of a HIPE formulation as the discrete phase in a microfluidic setup to obtain functional, monodisperse poly(HIPE) beads, has never been exploited. The closest report to such an approach is the generation of sessile droplets of HIPE from a needle in air and their subsequent detachment and polymerization.<sup>27</sup> The droplet breakup occurs as an interplay between interfacial tension and gravity, and although control of droplet size is achieved, large droplets with sizes of the order of the capillary length are formed, resulting in poly(HIPE) beads as large as 2 mm in diameter.

## Results and Discussion

We investigated the production of porous polymer beads using a high internal phase emulsion (HIPE) as the basis to generate pores within the beads and a simple microfluidic setup<sup>36,37</sup> for droplet generation composed of a tubing and needles (Figure 1), in order to avoid any labor-intensive device preparation techniques such as soft lithography.<sup>38</sup> An aqueous continuous carrier phase was introduced using a syringe pump from the inlet of the transparent tubing. A needle was inserted perpendicularly into this tubing. The monomer-based HIPE mixture was fed with a controlled rate using the second syringe pump. The original setup

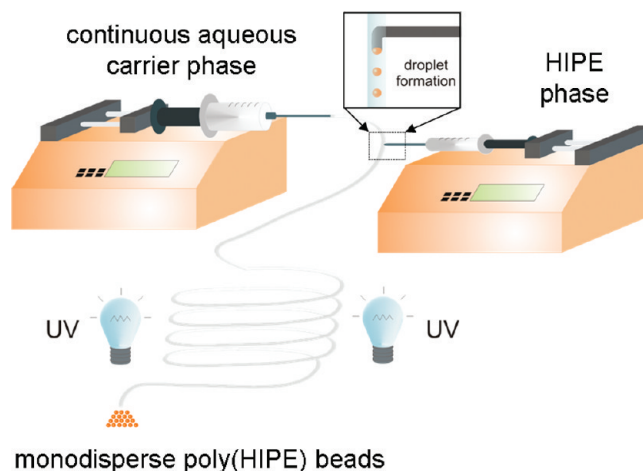


**Figure 1.** Tubing-needle-based simple microfluidic setup used in this study for production of poly(HIPE) particles.

of this simple approach as reported by McQuade et al.<sup>37</sup> did not always provide monodisperse droplets. We therefore aligned the exit of the needle with the direction of flow of the continuous phase by bending the needle tip 90°, effectively transforming the system from a T-junction into a coflow device.<sup>36</sup> Droplet formation occurred as a result of the large difference in pumping rates between the continuous and discrete phases. Addition of surfactant to the continuous aqueous carrier phase seemed crucial for stabilizing and carrying the HIPE droplets (now being a W/O/W emulsion) on their journey through the tubing. Solidification of the droplets in the downstream part of the tubing was achieved via photopolymerization, an approach that was recently introduced in conventional poly(HIPE) synthesis.<sup>20</sup> Photoinitiation was preferred over its thermal equivalent, as heating is known to destabilize HIPE formulations, especially those with limited polarity differences between the two phases.<sup>19</sup>

Initially, HIPE formulations were prepared from highly hydrophobic acrylate monomers. Typically, the HIPE formulation consisted of 90% internal water phase (0.1 M aqueous NaCl solution) and 10% continuous reactive oil phase, which contains a solution of a photoinitiator (4 wt %) in 2-ethylhexyl acrylate (EHA, 65 vol %), di(ethylene glycol) diacrylate (15 vol %), and the surfactant Span 80 (20 vol %). An aqueous solution of sodium dodecyl sulfate (SDS, 3%) was used as the continuous carrier phase in the microfluidic device. Under these conditions, nonspherical poly(HIPE) segments were obtained (Figure S1 in the Supporting Information). The high viscosity of the HIPE led to a jetting rather than dripping regime, with the cylindrical jet of HIPE being broken up as a result of a Plateau–Rayleigh instability. The formed HIPE segments were of too high viscosity to adjust to a spherical lowest-surface-area droplet. Intriguing fibril-like side filaments were observed. These preliminary results were exciting as there is a growing interest in nonspherical particles<sup>39,40</sup> such as rods<sup>41–43</sup> due to their unique packing, self-assembly, and mechanical properties. Nonspherical particles or droplets can easily be prepared in microfluidic devices, but the key in all cases is the use of a confined space, determining the final shape of the droplets or particles. The present case is different in that the nonspherical shape is directly correlated to the viscous behavior of the HIPE phase. We therefore took an interest in optimizing the process in order to improve control of the shape of the nonspherical segments.

Reducing the pumping rate of the HIPE phase resulted in a decreased average length of the obtained irregular segments. Attempts to improve the regularity of the obtained nonspherical structures, including a reduction of the internal water phase to 80% of the HIPE or changing EHA with lauryl acrylate



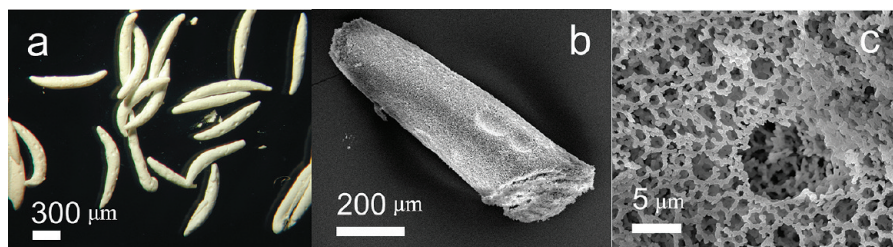


**Figure 2.** Poly(HIPE) rods. (a) Optical microscopy image showing uniformity and SEM images of (b) a partial rod and (c) surface of a rod.

did not result in any improvement. Further trials to increase the viscosity of the continuous phase by using 80% glycerol in water<sup>44</sup> as the continuous phase or decreasing the viscosity of the HIPE phase, by changing the surfactant that was used for the HIPE preparation to ABIL EM 90, did not improve the process either.

However, a different HIPE formulation<sup>45</sup> dramatically improved the regularity and reproducibility of the nonspherical segments, now showing resemblance with rods. 2,2-Dimethoxy-2-phenylacetophenone (DMPA, 33 mg) was dissolved in a mixture of ethylene glycol dimethacrylate (EGDMA, 0.34 mL), glycidyl methacrylate as functional monomer (GMA, 0.51 mL), and a polymeric surfactant, i.e., poly(ethylene oxide)-*b*-poly(propylene oxide)-*b*-poly(ethylene oxide) (PEO-PPO-PEO, MW 4400, 0.15 mL). Addition of 3.6 mL of aqueous  $\text{CaCl}_2 \cdot 2\text{H}_2\text{O}$  solution (1.3 wt %) to this oil phase resulted in 78% internal aqueous phase in the final HIPE, which was viscous. In our coflow device, porous uniform poly(HIPE) rods (Figure 2) were fabricated. To our knowledge, direct preparation of nonspherical poly(HIPE) particles has not been reported so far. Moreover, the preparation of nonspherical particles with a diameter ( $\sim 0.2$  mm) considerably smaller than the dimension of the continuous channel (0.8 mm inner diameter) and dictated by the viscosity of the dispersed phase is unprecedented.

When the molecular weight of the surfactant PEO-PPO-PEO was decreased to 2800 g/mol, a HIPE of low viscosity was obtained. This enabled us to produce nearly spherical droplets of HIPE and the corresponding poly(HIPE) beads. While the use of SDS solution as the carrier phase yielded polydisperse beads, monodisperse beads were obtained using an aqueous poly(vinyl alcohol) solution (PVA, 3%) (Figure 3).

SEM images of the obtained beads show that the pores are predominantly micrometer-sized (as we aimed for) reaching up to  $15\text{ }\mu\text{m}$ . In addition, it is important to stress that the beads show no “skin” effect. The undesired “skin” effect, which prevents reagents to penetrate into the porous inner part, is often observed in the preparation of porous beads by conventional methods involving a porogen.<sup>46</sup> In our case, the pores resulted from the 78% internal aqueous phase in the HIPE formulation, which can be increased up to  $\sim 87\%$  if spherical bead formation is desired. Above this limit, the HIPE phase becomes too viscous, preventing proper droplet breakup. The surface area of the obtained beads was determined as low as  $16\text{ m}^2/\text{g}$ , which is not surprising for poly(HIPE).<sup>8</sup> The poly(HIPE) beads exhibited an approximate diameter of  $400\text{ }\mu\text{m}$ , which is 5-fold smaller compared to the previously reported monodisperse poly(HIPE) beads.<sup>27</sup> We want to emphasize the importance of the coflow geometry (bent needle) for obtaining monodisperse poly(HIPE) beads instead of a T-junction (straight needle) as originally reported. Monomer conversion for the poly(HIPE) beads exceeded 75%, which is roughly 2-fold higher when compared to beads prepared with the conventional porogen method. This result indicates a good stability of the HIPE formulation during the second emulsification process in the microfluidic channel, to give a water-in-oil-in-water double emulsion.

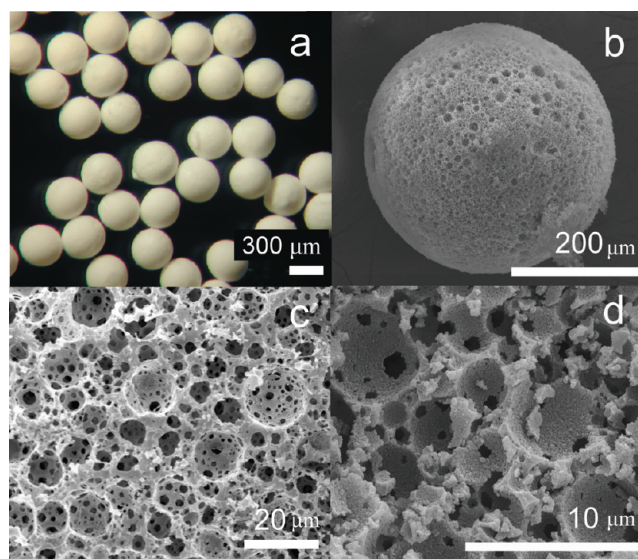


**Figure 3.** Porous, size-monodisperse near-spherical poly(HIPE) beads: (a) optical microscopy image showing size monodispersity; SEM images of (b) a whole bead, (c) surface of a bead, and (d) inner part of a broken bead.

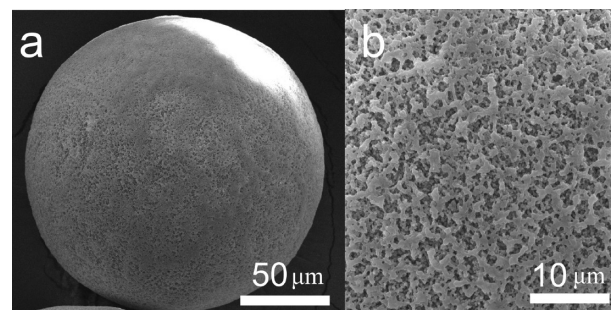


**Figure 4.** SEM images of “classical” macroporous beads prepared using porogens: (a) a whole bead; (b) surface of the same bead.

In addition to the monomer conversion, poly(HIPE) beads are compared with “classical” porous beads that we prepared using the same microfluidic setup. In contrast to the poly(HIPE) beads where water droplets act as the pore forming inert ingredient, “classical” macroporous beads are prepared by adding a porogen or a mixture of porogens to the initial monomer mixture. During polymerization, the solubility of the growing polymer chains decreases and phase separation occurs between polymer and the porogen/monomer mixture. Final macropores are obtained after removal of the porogen by washing. Pores of the beads obtained via this route are much smaller (Figure 4) compared to the pores of the poly(HIPE) beads (Figure 3). It is worth mentioning that an accompanying advantage of the HIPE pathway is the elimination of the use of organic porogens, thanks to the water-in-oil emulsion template.

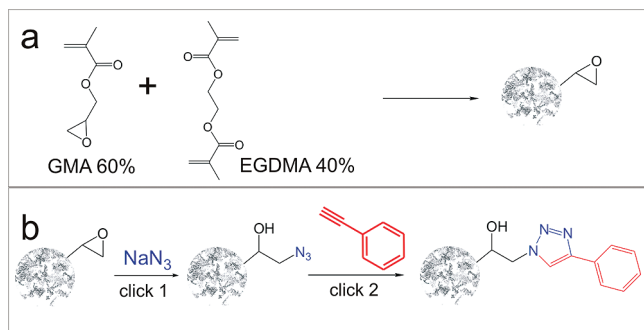


**Figure 5.** Synthesis and “click”–“click” modification of both poly(HIPE) and “classical” beads. (a) Monomer and cross-linker used in the synthesis of the beads. (b) Schematic representation of the serial “click” reactions.

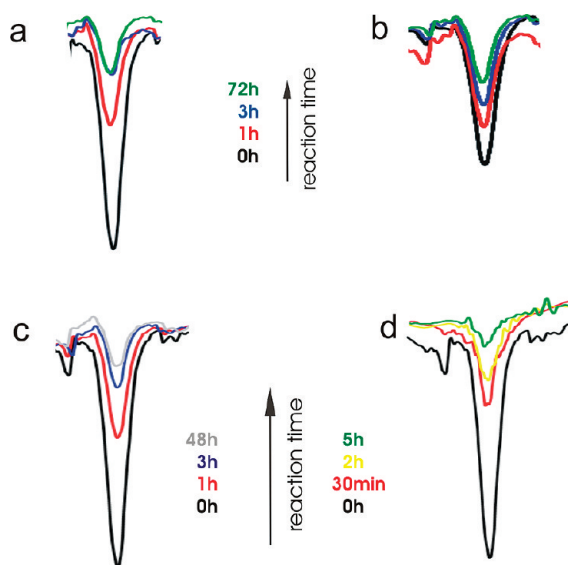


**Figure 6.** Monitoring  $\text{--N}_3$  peaks during CuAAC reactions: (a) poly(HIPE) beads/ $\text{CuSO}_4$ , (b) “classical” beads/ $\text{CuSO}_4$ , (c) poly(HIPE) beads/ $\text{CuBr}$ , (d) poly(HIPE) beads/ $\text{CuBr}$  at 50 °C. The IR spectra were normalized with respect to the carbonyl peaks (full spectra are available in the Supporting Information).

Next, we explored chemical postfunctionalization of the poly(HIPE) beads by using the epoxy groups that originated from the glycidyl methacrylate (GMA) monomer (Figure 5). The epoxy group allows a two-step “click”–“click”<sup>47</sup> process,<sup>1,22,48</sup> which involves ring-opening of the epoxy groups with  $\text{NaN}_3$  to introduce azide groups, followed by a Cu catalyzed cycloaddition to the azide by alkynes (CuAAC, Figure 5b).<sup>49</sup> Using phenyl acetylene as a model compound, we compared the performance of poly(HIPE) beads and “classical” macroporous beads. Although the surface area of these “classical” beads was 49  $\text{m}^2/\text{g}$  (3 times higher than that of poly(HIPE) beads), they were outperformed by poly(HIPE) beads in terms of reaction rates in CuAAC (Figure 6a,b), which was revealed by comparing the change in the azide signal located at 2100  $\text{cm}^{-1}$  in ATR-IR spectra as a function of time. The same trend was observed when the reaction was performed with  $\text{CuBr}$  catalyst at room temperature and at 50 °C (Figure 6c,d). In the latter case, more than 90% of the azide peak disappeared in only 5 h, meaning near-quantitative triazole formation, which is remarkable taking into account the rather high azide loading (0.81 mmol/g obtained from elemental analysis). It is also important to mention that poly(HIPE) beads have more azide groups than the “classical” beads, indicating that even the first “click” reaction is more efficient for poly(HIPE) beads. Elemental analysis confirmed the difference in azide loading: 0.81

and 0.31 mmol/g for poly(HIPE) and “classical” beads, respectively. This performance is attributed to the large macroporous open cellular structure of the poly(HIPE) beads, with excellent accessibility of the functional groups. These results indicate that poly(HIPE) beads can serve as a universal platform for “clicking” compounds of interest such as biomolecules, drugs, and catalysts.

## Conclusion

We showed the fabrication of monodisperse submillimeter poly(HIPE) beads and rods by using a simple microfluidic coflow device. In obtaining the nonspherical shapes, the viscosity of the emulsified HIPE phase played a crucial role. Creating nonspherical particles in microfluidics by means other than using the channel dimensions is unprecedented to the best of our knowledge. Our microfluidic approach allows for the fabrication of submillimeter-sized monodisperse spherical poly(HIPE) beads (diameter of about 400  $\mu\text{m}$ ), which is 5 times smaller than thus far reported using the sessile drop approach.<sup>27</sup> The porous polymer particles made using HIPE have pore sizes that are much larger than that of common macroporous beads prepared using porogens. We demonstrated that postfunctionalization of poly(HIPE) beads is easily achieved by a consecutive “click”–“click” approach. Thanks to their macroporous structure, the efficiency of the click reactions for poly(HIPE) beads was considerably higher than for “classical” macroporous beads, despite the latter having a 3-fold higher total surface area. We envisage that these poly(HIPE) beads open new possibilities in several fields such as separation science, solid-supported peptide synthesis, catalysis, and scavenging.

## Experimental Section

**Materials.** Solvents used for the bead wash procedure were technical grade and used as received.  $\text{H}_2\text{O}$  used was MilliRO grade. Dimethyl sulfoxide (DMSO), 2,2-dimethoxy-2-phenylacetophenone (DMPA), poly(vinyl alcohol) (PVA, 95% hydrolyzed, 95000 MW),  $\text{NaN}_3$ , DMF, sodium ascorbate ( $\text{NaOAsc}$ ),  $\text{CuSO}_4$ , and ethylene glycol dimethacrylate (EGDMA) were purchased from Acros Organics. PVC tubing (1.6 mm inner diameter), glycidyl methacrylate (GMA), dichloromethane (DCM), tripropargylamine, poly(ethylene oxide)-*b*-poly(propylene oxide)-*b*-poly(ethylene oxide) (PEO-PPO-PEO) surfactants, basic  $\text{Al}_2\text{O}_3$ , 2-ethylhexyl acrylate (EHA), benzyl bromide, phenylacetylene, di(ethylene glycol) diacrylate (DEGDA, technical grade), 2-benzyl-2-(dimethylamino)-4'-morpholinobutyrophenone (BDM), lauryl acrylate, cyclohexanol, dodecanol, and  $\text{CuBr}$  were purchased from Sigma-Aldrich. Synthesis of benzyl azide was reported elsewhere.<sup>50</sup> ABIL EM 90 was kindly donated by Evonik Degussa. Both EGDMA and GMA were passed over basic  $\text{Al}_2\text{O}_3$  prior to use.  $\text{CuBr}$  was washed with glacier acetic acid overnight to remove oxidized species, further washed with ethanol and DEE, and dried under vacuum. Tygon tubing (0.8 mm internal diameter, Saint Gobain Plastics) was purchased from VWR International. 22G blunt needles were purchased from Hamilton. 30G disposable needles were purchased from Becton Dickinson and blunted. PVA solution was prepared by stirring the corresponding amount of PVA in water that was heated up to 70–80 °C. The elevated temperature was kept until all polymer is dissolved, and then the solution was cooled down. No precipitation was observed.

**Instrumentation.** Scanning electron microscopy (SEM) images were recorded with a Quanta 200 FEG FEI scanning electron microscope operated at an acceleration voltage of 5 kV. Samples were sputtered with gold prior to SEM analysis. Optical microscopy images were recorded with a Nikon SMZ800 microscope. FTIR spectra were recorded by a Perkin-Elmer Spectrum 1000 equipped with an ATR probe.  $\text{N}_2$  sorption isotherms were



measured on a Belsorp-Mini II apparatus at 77 K. The surface area was calculated using the BET method.  $^1\text{H}$  NMR spectra were recorded by a Bruker Avance 300 spectrometer. Elemental analysis measurements were done in CNRS Paris. Overhead stirrer was an IKA RW 20 DZM. Syringe pumps used were KDS Scientific and New Era NE-300 model. A Metalight UV box operating with 12 (320–400 nm) lamps was used for solidification.

**Preparation of Poly(HIPE) Beads.** In a typical procedure, DMPA (33 mg) was dissolved in a mixture of EGDMA (0.34 mL), GMA (0.51 mL), and PEO–PPO–PEO 2800 (0.15 mL) in a 50 mL flask that was covered with a piece of aluminum foil to avoid light penetration. While this mixture is being stirred at 350–400 rpm by an overhead stirrer equipped with a Teflon propeller that fits to the bottom of the flask, aqueous  $\text{CaCl}_2 \cdot 2\text{H}_2\text{O}$  solution (3.6 mL, 1.3% wt) was added dropwise for 30–40 min. When the addition was complete, the flask was lowered and stirring was kept on the upper part of the emulsion for an additional 5–10 min to ensure homogenization (other HIPEs mentioned in the text were prepared in a similar fashion). This mixture was polymerized in the microfluidic device with a pumping rate of  $0.20 \text{ mL h}^{-1}$  using a 30G blunt needle. The continuous carrier phase was aqueous PVA solution (3% weight) pumped with a rate of  $1.20 \text{ mL min}^{-1}$ . 0.5 m PVC tubing was used, which enabled the formed HIPE droplets to be exposed to UV light for  $\sim 15 \text{ s}$  on-flight. Further off-tubing UV curing was performed for at least 15 min for further polymerization. Obtained beads were washed on a glass filter with warm  $\text{H}_2\text{O}$ , DCM, MeOH, DCM, and DEE and dried under vacuum at room temperature overnight.

**Preparation of Poly(HIPE) Rods.** Rods were prepared in the same way as the beads. Differences were the surfactant (PEO–PPO–PEO 4400), tubing (0.5 m Tygon), needle (22G), continuous phase pumping rate ( $15.0 \text{ mL h}^{-1}$ ), and the HIPE phase pumping rate ( $0.80 \text{ mL h}^{-1}$ ).

**Preparation of “Classical” Porous Beads.** Briefly, BDM (16 mg) was dissolved in a solution of EGDMA (0.16 mL), GMA (0.24 mL), and a 4:1 volume mixture of cyclohexanol and dodecanol (0.60 mL). This homogeneous mixture was emulsified in our microfluidic setup as the discrete phase. Carrier phase was SDS solution. Tygon tubing (2 m, 0.8 mm i.d.) and 30G blunt needle was used. Pumping rates were  $1.3 \text{ mL/min}$  and  $0.8 \text{ mL/h}$  for continuous and discrete phases, respectively. After washing, obtained beads were analyzed by SEM, optical microscopy, and  $\text{N}_2$  sorption.

**Synthesis of Tris(benzyltriazolylmethyl)amine (TBTA).** On the basis of a reported procedure,<sup>51</sup> TBTA was synthesized as follows: tripropargylamine (1 mL, 7.1 mmol), benzyl azide (3.14 g, 23.6 mmol),  $\text{CuSO}_4 \cdot 5\text{H}_2\text{O}$  (0.29 g, 1.2 mmol), and NaOAsc (0.68 g, 3.4 mmol) were added into a mixture of DCM (20 mL) and  $\text{H}_2\text{O}$  (20 mL), and reaction was performed by stirring for 24 h at room temperature.  $\text{H}_2\text{O}$  phase was washed with DCM ( $3 \times 20 \text{ mL}$ ); DCM phases were all combined and dried over  $\text{MgSO}_4$ . Product was purified by column chromatography using silica gel and MeOH:EtOAc (1:9) mixture as the eluent. White solid is obtained with 70% yield.  $^1\text{H}$  NMR ( $\text{CDCl}_3$ ):  $\delta$  (ppm) = 3.70 (s, 6H), 5.45 (s, 6H), 7.10–7.36 (15H), 7.60 (s, 3H) which fits with the original report.<sup>52</sup>

**Epoxy–Azide Conversion for Beads.** This conversion was done according to the literature.<sup>48</sup> Briefly, dried poly(HIPE) beads (50 mg) were preswollen in DMF (7 mL) in a flask,  $\text{NaN}_3$  (0.25 g) and  $\text{NH}_4\text{Cl}$  (0.21 g) were added, and the reaction took place for 24 h at  $50^\circ\text{C}$  while the flask is being rotated with a rotary evaporator motor.<sup>1</sup> Beads were washed on a glass filter with warm  $\text{H}_2\text{O}$ , DMF, MeOH, DCM, and DEE and dried under vacuum at room temperature overnight. Introduction of azide groups was confirmed by IR spectroscopy with the characteristic azide band at  $2100 \text{ cm}^{-1}$ . Same was applied to the “classical” beads.

**CuAAC Reactions on Azide-Containing Beads.**  $\text{CuSO}_4$ . Poly(HIPE) beads (10 mg) were added into a syringe fitted with a frit, and a solution of TBTA (4.8 mg),  $\text{CuSO}_4$  (1.12 mg), NaOAsc (1.78 mg), and phenylacetylene (25  $\mu\text{L}$ ) in  $\text{DMSO:H}_2\text{O}$  (0.5 mL, 4:1) was added. The syringe reactor was gently shaken by a vortex mixer. Samples were taken with time intervals and washed with acetone,  $\text{H}_2\text{O}$ , acetone, and DEE. Same was applied to the “classical” azido beads.

$\text{CuBr}$ . Poly(HIPE) beads (10 mg) were added into a syringe fitted with a frit, and a solution of TBTA (4.8 mg),  $\text{CuBr}$  (6.5 mg), and phenylacetylene (25  $\mu\text{L}$ ) in DMF (0.75 mL) was added. The syringe reactor was gently shaken by a vortex mixer. Samples were taken with time intervals and washed with acetone,  $\text{H}_2\text{O}$ , acetone, and DEE.

$\text{CuBr} + 50^\circ\text{C}$ . Poly(HIPE) beads (10 mg) were added into a 5 mL flask, and a solution of TBTA (4.8 mg),  $\text{CuBr}$  (6.5 mg), and phenylacetylene (25  $\mu\text{L}$ ) in DMF (0.75 mL) was added. The flask was placed in an oil bath that is heated up to  $50^\circ\text{C}$  and rotated by a rotary evaporator motor. Samples were taken with time intervals and washed with acetone,  $\text{H}_2\text{O}$ , acetone, and DEE.

**Acknowledgment.** This work has been financially supported by a Marie Curie Early Stage Research Training Fellowship of the European Community's Sixth Framework Program under Contract 020643 (M.T.G., Sendichem project), the Fund for Scientific Research–Flanders (FWO) (W.V.C.), EPSRC (P.J. C.), and The Belgian Program on Interuniversity Attraction Poles initiated by the Belgian State, Prime Minister's office (Program P6/27). The authors thank Attyah S. Alzhrani for SEM analysis of the nonspherical poly(HIPE) beads and Dr. H. Zhang (University of Liverpool) for the useful discussions.

**Supporting Information Available:** Procedure and SEM images of initial poly(HIPE) segments, full IR spectra for CuAAC reactions, and a video showing bead and rod manufacture. This material is available free of charge via the Internet at <http://pubs.acs.org>.

## References and Notes

- (1) Slater, M.; Snaiko, M.; Svec, F.; Frechet, J. M. J. *Anal. Chem.* **2006**, *78*, 4969–4975.
- (2) Fontanals, N.; Marce, R. M.; Cormack, P. A. G.; Sherrington, D. C.; Borrull, F. J. *Chromatogr. A* **2008**, *1191*, 118–124.
- (3) Hudson, D. J. *Comb. Chem.* **1999**, *1*, 333–360.
- (4) Prasada Rao, T.; Praveen, R. S.; Daniel, S. *Crit. Rev. Anal. Chem.* **2004**, *34*, 177–193.
- (5) Leeb, L.; Gmeiner, P.; Löber, S. *QSAR Comb. Sci.* **2007**, *26*, 1145–1150.
- (6) Miletic, N.; Vukovic, Z.; Nastasovic, A.; Loos, K. J. *Mol. Catal. B: Enzym.* **2009**, *56*, 196–201.
- (7) Haag, R.; Roller, S. *Top. Curr. Chem.* **2004**, *242*, 1–42.
- (8) Okay, O. *Prog. Polym. Sci.* **2000**, *25*, 711–779.
- (9) Poschalko, A.; Rohr, T.; Gruber, H.; Bianco, A.; Guichard, G.; Briand, J.-P.; Weber, V.; Falkenhagen, D. J. *Am. Chem. Soc.* **2003**, *125*, 13415–13426.
- (10) Guyomard, A.; Fournier, D.; Pascual, S.; Fontaine, L.; Bardeau, J.-F. *Eur. Polym. J.* **2004**, *40*, 2343–2348.
- (11) Garcia-Diego, C.; Cuellar, J. *Ind. Eng. Chem. Res.* **2005**, *44*, 8237–8247.
- (12) Crevecoeur, J. J.; Nelissen, L.; Lemstra, P. J. *Polymer* **1999**, *40*, 3685–3689.
- (13) Crevecoeur, J. J.; Nelissen, L.; Lemstra, P. J. *Polymer* **1999**, *40*, 3691–3696.
- (14) Hatate, Y.; Uemura, Y.; Ijichi, K.; Kato, Y.; Hano, T.; Baba, Y.; Kawano, Y. *J. Chem. Eng. Jpn.* **1995**, *28*, 656–659.
- (15) Dowling, P. J.; Goodwin, J. W.; Vincent, B. *Colloids Surf., A* **2001**, *180*, 301–309.
- (16) Cameron, N. R.; Sherrington, D. C. *Adv. Polym. Sci.* **1996**, *126*, 163–214.
- (17) Barbetta, A.; Cameron, N. R. *Macromolecules* **2004**, *37*, 3188–3201.

- (18) Krajnc, P.; Leber, N.; Brown, J. F.; Cameron, N. R. *React. Funct. Polym.* **2006**, *66*, 81–91.
- (19) Ruckenstein, E. *Adv. Polym. Sci.* **1997**, *127*, 1–58.
- (20) Pierre, S. J.; Thies, J. C.; Dureault, A.; Cameron, N. R.; van Hest, J. C. M.; Carrette, N.; Michon, T.; Weberskirch, R. *Adv. Mater.* **2006**, *18*, 1822–1826.
- (21) Zhang, H.; Cooper, A. I. *Soft Matter* **2005**, *1*, 107–113.
- (22) Cummins, D.; Duxbury, C. J.; Quaedflieg, P. J. L. M.; Magusin, P. C. M. M.; Koning, C. E.; Heise, A. *Soft Matter* **2009**, *5*, 804–811.
- (23) Li, N.-H.; Benson, J. R.; Kitagawa, N. US Patent 5,760,097, **1998**.
- (24) Cooper, A. I.; Zhang, H. US Patent 7,153,572, **2006**.
- (25) Zhang, H.; Hardy, G. C.; Rosseinsky, M. J.; Cooper, A. I. *Adv. Mater.* **2003**, *15*, 78–81.
- (26) Desforges, A.; Arpontet, M.; Deleuze, H.; Mondain-Monval, O. *React. Funct. Polym.* **2002**, *53*, 183–192.
- (27) Zhang, H.; Cooper, A. I. *Chem. Mater.* **2002**, *14*, 4017–4020.
- (28) Stefanec, D.; Krajnc, P. *React. Funct. Polym.* **2005**, *65*, 37–45.
- (29) Stefanec, D.; Krajnc, P. *Polym. Int.* **2007**, *56*, 1313–1319.
- (30) Dubinsky, S.; Zhang, H.; Nie, Z.; Gourevich, I.; Voicu, D.; Deetz, M.; Kumacheva, E. *Macromolecules* **2008**, *41*, 3555–3561.
- (31) Wan, J.; Bick, A.; Sullivan, M.; Stone, H. A. *Adv. Mater.* **2008**, *20*, 3314–3318.
- (32) Tan, W.-H.; Takeuchi, S. *Adv. Mater.* **2007**, *19*, 2696–2701.
- (33) Utada, A. S.; Chu, L.-Y.; Fernandez-Nieves, A.; Link, D. R.; Holtze, C.; Weitz, D. A. *MRS Bull.* **2007**, *32*, 702–708.
- (34) Xu, S.; Nie, Z.; Seo, M.; Lewis, P.; Kumacheva, E.; Stone, H. A.; Garstecki, P.; Weibel, D. B.; Gitlin, I.; Whitesides, G. M. *Angew. Chem., Int. Ed.* **2005**, *44*, 724–728.
- (35) Nie, Z.; Park, J. I.; Li, W.; Bon, S. A. F.; Kumacheva, E. *J. Am. Chem. Soc.* **2008**, *130*, 16508–16509.
- (36) Gokmen, M. T.; De Geest, B. G.; Hennink, W. E.; Du Prez, F. E. *ACS Appl. Mater. Interfaces* **2009**, *1*, 1196–1202.
- (37) Quevedo, E.; Steinbacher, J.; McQuade, D. T. *J. Am. Chem. Soc.* **2005**, *127*, 10498–10499.
- (38) Becker, H.; Gärtner, C. *Anal. Bioanal. Chem.* **2008**, *390*, 89–111.
- (39) Kim, J. W.; Larsen, R. J.; Weitz, D. A. *Adv. Mater.* **2007**, *19*, 2005–2009.
- (40) Dendukuri, D.; Pregibon, D. C.; Collins, J.; Hatton, T. A.; Doyle, P. S. *Nat. Mater.* **2006**, *5*, 365–369.
- (41) Bon, S. A. F.; Mookhoek, S. D.; Colver, P. J.; Fischer, H. R.; van der Zwaag, S. *Eur. Polym. J.* **2007**, *43*, 4839–4842.
- (42) Gross, G. A.; Hamann, C.; Günther, P. M.; Köhler, J. M. *Chem. Eng. Technol.* **2007**, *30*, 341–346.
- (43) Zhou, W. Z.; Cao, J.; Liu, W. C.; Stoyanov, S. *Angew. Chem., Int. Ed.* **2009**, *48*, 378–381.
- (44) Steinbacher, J. L.; Moy, R. W. Y.; Price, K. E.; Cummings, M. A.; Roychowdhury, C.; Buffly, J. J.; Olbricht, W. L.; Haaf, M.; McQuade, D. T. *J. Am. Chem. Soc.* **2006**, *128*, 9442–9447.
- (45) Krajnc, P.; Leber, N.; Stefanec, D.; Kontrec, S.; Podgornik, A. *J. Chromatogr., A* **2005**, *1065*, 69–73.
- (46) Dubinsky, S.; Park, J. I.; Gourevich, I.; Chan, C.; Deetz, M.; Kumacheva, E. *Macromolecules* **2009**, *42*, 1990–1994.
- (47) Kolb, H. C.; Finn, M. G.; Sharpless, K. B. *Angew. Chem., Int. Ed.* **2001**, *40*, 2004–2021.
- (48) Tsarevsky, N. V.; Bencherif, S. A.; Matyjaszewski, K. *Macromolecules* **2007**, *40*, 4439–4445.
- (49) Wu, P.; Fokin, V. V. *Aldrichim. Acta* **2007**, *40*, 7–17.
- (50) Bonami, L.; Van Camp, W.; Van Rijckegem, D.; Du Prez, F. E. *Macromol. Rapid Commun.* **2009**, *30*, 34–38.
- (51) Lee, B.-Y.; Park, S. R.; Jeon, H. B.; Kim, K. S. *Tetrahedron Lett.* **2006**, *47*, 5105–5109.
- (52) Chan, T. R.; Hilgraf, R.; Sharpless, K. B.; Fokin, V. V. *Org. Lett.* **2004**, *6*, 2853–2855.